Journal of Materials Chemistry A

The Impact of Radical Loading and Oxidation on the Conformation of Organic Radical Polymers by Small Angle Neutron Scattering

Journal:	*Journal of Materials Chemistry A*
Manuscript ID	TA-ART-05-2018-004583.R1
Article Type:	Paper
Date Submitted by the Author:	02-Jul-2018
Complete List of Authors:	Martin, Halie; University of Tennessee, Chemistry Hughes, Barbara; National Renewable Energy Laboratory Braunecker, Wade; National Renewable Energy Laboratory, Gennett, Thomas; NREL, Dadmun, Mark; University of Tennessee, Chemistry

The Impact of Radical Loading and Oxidation on the Conformation of Organic Radical Polymers by Small Angle Neutron Scattering

Halie J. Martin[1], Barbara Hughes[2], Wade A. Braunecker[2], Thomas Gennett[2,3], and Mark D. Dadmun[1,4*]

1. Department of Chemistry, University of Tennessee, Knoxville, Tennessee
2. Chemical and Materials Science, National Renewable Energy Laboratory, Golden, CO
3. Department of Chemistry, Colorado School of Mines, Golden, CO
4. Chemical Sciences Division, Oak Ridge National Lab, Oak Ridge, Tennessee

*Email - dad@utk.edu

Abstract

Electrodes comprised of organic polymeric materials containing stable radicals have become attractive for incorporation into organic radical batteries. Specifically, the radical polymer poly(2,2,6,6-tetramethylpeperidinyloxy-4-yl methacrylate) (PTMA) exhibits extremely rapid electron charge transport rates, comparable to traditional transition metal ions. However, the structural reorganization that the polymer undergoes during charging is not well understood. Using small angle neutron scattering, we have investigated the structural changes the PTMA polymer exhibits with variation of radical concentration or oxidation. The results indicate that as the radical concentration is increased, the polymer becomes more inflexible and begins to aggregate with neighboring polymer chains as the radicals on the polymer align with neighboring solvated chains. Additional studies monitor the conformational changes of the PTMA copolymers with oxidation to mimic the structural changes that the polymer undergoes during charging. These results show that polymers with low radical densities are more susceptible to reorientation with charging than a polymer that is fully saturated with radical moieties. This study therefore provides seminal fundamental information that identifies the relationship between radical density and

molecular structure providing crucial insight that is needed to improve the performance of organic radical batteries.

Introduction

Organic radical batteries, ORBs, are novel devices that are coming to the forefront of research after being first developed in the early 2000s. ORBs incorporate organic radical cathode materials into the battery and are designed to be an alternative to traditional inorganic based materials in Lithium-ion batteries.[1] Lightweight Li-ion batteries are commonly found in cellular phones, laptop computers, and other electronic devices. These rechargeable Li-ion batteries have dominated personal electronics for the past few decades.[2] Mass produced Li-ion batteries traditionally use transition metal based cathode materials such as manganese, iron, and nickel which are often expensive to manufacture, result in poor recycling of consumed materials, have limited capacities, are potentially toxic, as well as not being environmentally friendly by using precious, unrenewable mineral materials.[3–6] It is also difficult to improve further their already high specific capacity, or simply the amount of discharge over time of the battery, with these cathode materials. Alternative active materials such as conducting polymers and disulfide compounds have attained desired capacities for Li-ion based batteries.[2] A general requirement for improved battery technology is the potential for high-power density, or improvement in the reversible charge per unit weight.[7] A significant hurdle to increase energy storage in new batteries is finding a suitable blend of redox materials that attain long-term cycling stability with fast, stable, and reversible redox reactions.[8] Thus, ORBs with organic radical electrode materials offer devices with increased energy and power density, as well as similar cycling stability as batteries with popular inorganic cathode materials. ORBs have the potential to become a popular and environmentally friendly form of energy storage.[3,4]

Organic polymeric material is abundant and can be easily synthesized. Research to maximize the incorporation of these materials into batteries has increased significantly over the last decade. More specifically, polymers containing stable organic radicals have become popular and extensively studied for applications ranging from photochemical applications to biological labeling, and polymeric stabilizers, and smart card materials.[4,5,9] Polyradicals, a polymer with unpaired electrons, are more advantageous than other organic electrode materials including polythiophenes, poly(acetylene), and organosulfur compounds because these polyradicals have unique redox properties.[10] Polyradicals have two main components: a polymer backbone and a robust radical side group. The neutral polyradicals are unusually stable materials that can undergo reversible redox reactions allowing for easy and fast conversion between the anionic, or negative, and cationic, or positive state.[5,11] This unique property can transform an insulating polymer into a conducting polymer capable of electron transport properties similar to inorganic materials currently incorporated into Li-ion batteries.[8,12] The incorporation of polyradical, organic materials in an active redox layer used in batteries are also attractive due to their eco-friendliness.[3,13] Prototype organic radical batteries have been produced by the NEC Corporation and tested with polymer/electrode thicknesses thinner than 50μm where the densely populated components exhibited unusually high specific capacities.[13] For these prototype materials of rechargeable batteries to be scaled-up, they must exhibit several characteristics including cell voltages above 2 Volts, cycle life greater than 3000 cycles, as well chemically stable for up to 15 years.[6]

The most popular and possibly most intriguing organic radical employed in battery research is 2,2,6,6-tetramethylpiperidine 1-oxyl (TEMPO) which readily undergoes reversible oxidation and reduction. TEMPO has a highly stable nitroxide radical that is used for many other applications such as spin labels for electron resonance to examine conformation, paramagnetic

studies, as well a popular oxidizing agents.[14,15] The stability of the nitroxide radical is a direct result of two important structural features: the N-O bond that is easily delocalized by an unpaired electron and four methyl groups neighboring the nitroxide bond increasing steric hindrance of the radicals.[8] The charging of this material through material swelling by an electrolyte results in electrons transferring through the polymer to form complexes.[3] The reversible oxidation and reduction of the nitroxide radical to either oxoammonium cation or to the aminoxyl anion results in either p-doping or n-doping of the polymeric material (Figure 1). When the material is discharged, the ion returns to the stable nitroxide radical, where the motion of the electrons through the electrode materials are characterized by a hopping mechanism.[3,16–18] TEMPO radicals are able to perform as either cathode or anode materials increasing the functionality of the polymer, however the anion is much less stable in typical carbonate electrolytes. Grafting of TEMPO units to a polymer backbone, such as poly(methyl methacrylate), creates a polymer, poly (2,2,6,6-tetramethylpeperidinyloxy-4-yl methacrylate) or PTMA, that will increase the specific charge of the polymer, or the number of electrons that can be stored per repeat unit/monomer of the polymer. When the p-type redox active material of PTMA is incorporated into fabricated layered architectures, the PTMA has exhibited life cycles greater than 1000 recharges, exhibits good chemical stability, and can operate at almost 100% of their theoretical capacity.[5,6,13,19] Therefore, coupled with lack of device degradation, nitroxide-radical based ORBs are very promising materials to improve the capacity of Li-ion batteries.

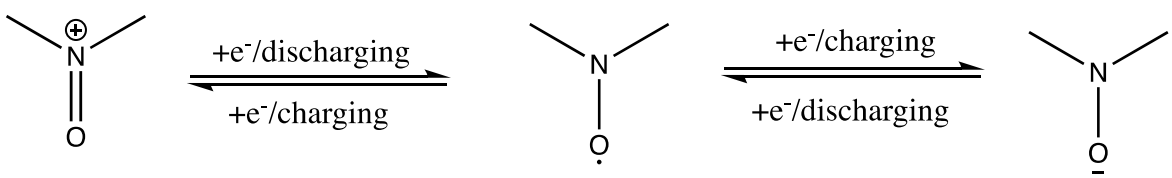

Figure 1: Reversible redox/oxidation of nitroxide radicals.

While, the potential of PTMA as an important component in organic radical batteries has increased over the past 6 years, further progress in this field is limited by minimal knowledge of the correlation of material efficiency and the conformational changes of the polymeric material during use. Previous research suggests that PTMA will undergo conformational changes and reorientation, rather than bond breaking, during the redox process due to the rapid charge transport kinetics that the material exhibits.[5] Kemper et al investigated the structural change of amorphous PTMA films through molecular dynamic simulations.[3] They determined that PTMA films assemble as an amorphous network of radicals in the solid film, which results in small distances between radicals on neighboring polymer chains that decrease with increasing radical loading.[5] Moreover, increasing the available nitroxide radicals on the polymer backbone increases the capacity of the system. Thus, increasing the number of TEMPO radicals on a poly(methyl methacrylate) backbone and establishing a morphological-performance relationship will enable the control and improvement of the performance of organic radical batteries.

With this in mind, small angle neutron scattering (SANS) was used to gain an in-depth understanding of the molecular structure-property relationships of the stable organic-radical polymeric redox-active materials PTMA. The neutron scattering analysis will first emphasize how the conformational structure of PTMA changes in the neutral radical state as the radical moiety density increases from 10% (PTMA-10) to a polymer with a radical on every monomer (PTMA-100). This is accomplished by increasing the amount of TEMPO pendant groups on the poly(methyl methacrylate) backbone. Examination of the conformation of the polymers is possible in dilute solution. These results indicate that as the loading of radicals onto the PTMA increases, the flexibility of the polymer decreases and the polymer begins to aggregate due to the radical moieties desire to "find" each other and align both inter- and intra-molecularly. The second

analysis examines the change in the polyradicals conformation during the oxidation and reduction cycles via electrolyte swelling with lithium hexafluoride, $LiPF_6$ for a polyradical with a small density of TEMPO pendant groups (PTMA-20) and a polyradical completely saturated with TEMPO pendant groups (PTMA-100). The SANS results of the charged PTMA-20 shows distinct conformation changes relative to the neutral state, which implies significant polymer rearrangement with the increase in oxoammonium cations. The SANS data also show that the charged PTMA-100 molecules do not show significant conformation variation as the polymer becomes further charged. These studies will provide insight that can be used to improve the performance of organic radical batteries by elucidating a molecular structure-performance relationship enhancing the knowledge of electron hopping transport of the polymer in solution.

Experimental

Synthesis

4-Methacryloyloxy-2,2,6,6-tetramethyl-piperidin-N-oxyl and its corresponding polymer, poly(4-methacryloyloxy-2,2,6,6-tetramethyl-piperidin-N-oxyl), (PTMA-100) were synthesized via group-transfer anionic polymerization following the literature procedure by Bugnon et al.[20] To synthesize the random copolymer of PTMA and PMMA to produce polymers with varying TEMPO content, the synthetic procedure was altered to include the appropriate molar ratios of TEMPO methacrylate and methyl methacrylate in the monomer feed. The model compounds are shown in Figure 2. To verify the composition of the TEMPO methacrylate copolymer, the charge capacity of a lithium half-cell was measured and agreed with the calculated capacity of the PTMA-X based on stoichiometry and film geometry following the procedure of Bobela et al.[7]

PTMA and LiPF6 in solution

In the oxidation of the PTMA-X samples, the correct amount of lithium hexafluoride, $LiPF_6$ powder for a 0.1M solution and the correct amounts of the soluble non-crosslinked PTMA samples to give xxmM solution were dissolved in 5mL of d_3–acetonitrile inside a helium filled dry box. Once completely dissolved, the solution was placed in a small 10 ml electrochemical reaction vessel with a working platinum foil basket, a frit isolated coiled platinum wire counter electrode and an Ag/AgCl reference electrode (Supplemental Figure S1). From the sample mass, the amount of coulombs were calculated that were needed to determine the appropriate amount oxidation of the sample based on the radical content. The programmed EG&G PAR 2273 potentiostat was set to stop when the correct coulomb count was met as normalized to the blank electrolyte solutions. The extent of oxidation was checked through normal pulse voltammetry. The solutions were then frozen on dry ice and stored in the dark until characterization to minimize any degradation.

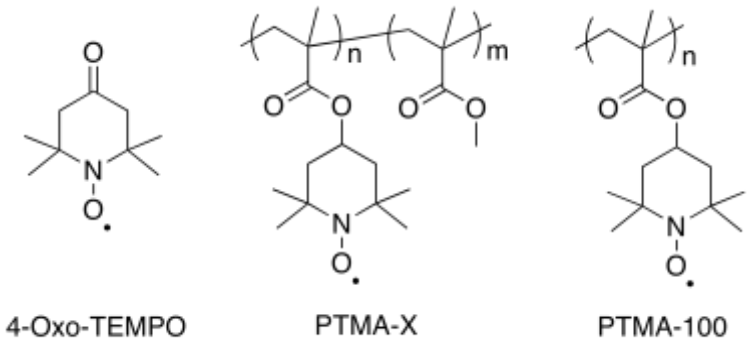

Figure 2: Structure of 4-oxo-TEMPO, PTMA-PMMA random copolymer, and PTMA-100 polymer.

Molecular Weight Determination for PTMA-X Samples

The molecular weight of the PTMA-X samples were determined using gel permeation chromatography (GPC) following literature procedure by Hughes et al.[5] In this procedure,

polymer samples were dissolved in HPLC-grade chloroform (concentration = 2mg/mL) and filtered using a 0.45μm PVDF filter. The GPC used two preparatory PL-Gel 300 x 25 mm (10μm) mixed D GPC columns in a connected series, an Agilent 1200 series autosampler, an inline degasser, and a diode array detector. The samples were measured at 25 °C with HPCL-chloroform for eluent at 10mL/min. The molecular weight and polydispersity of the polymer was determined using linear polystyrene standards (Supplemental Figure S2).

Small Angle Neutron Scattering

Small angle neutron scattering measurements of PTMA-X solutions in d_3-acetonitrile (d_3-MeCN) were performed at the GP-SANS instrument at the High Flux Isotope Reactor (HFIR) and at the EQ-SANS instrument at the Spallation Neutron Source (SNS), both at Oak Ridge National Laboratory (ORNL). For samples run at HFIR, the sample-to-detector distances used were 1.5m, 6.8m, and 19.2m with a wavelength of 4.7Å, which allowed a Q range of 0.0038-0.51Å^{-1}, where $Q = 4\pi/\lambda\sin(\theta/2)$; λ is the neutron wavelength, and θ is the scattering angle. The raw data were reduced using SPICE ORNL reduction protocol in Igor Pro.[21] Addition SANS experiments were performed at SNS where the sample-to-detector distances of 1.3m, 3m, and 8m was used with a spectrum of neutrons with wavelengths from 2.5 to 8 Å to provide a Q range of 0.0025-1Å^{-1}. Data reduction to produce I(Q) vs Q was performed according to the standard procedures implemented in the Mantid software to produced reduced absolute intensities.[22] Samples were mounted in 2mm wide quartz banjo cells. The raw data for both instruments were corrected for empty cell scattering, dark current, and detector sensitivity. Absolute coherent scattering was obtained by eliminating the contributions from background incoherent scattering from the quartz cell and normalized to a known standard.

Results

The scattering intensity, I(Q), for the neutral and charged PTMA polymers and copolymers were first fit to a flexible cylinder form factor, P(Q), with a polydisperse radius where the form factor is normalized to the volume of the cylinder (Equation 1).[23,24] The scale factor is set to the particle volume fraction in solution and the background is related to the incoherent scattering at high Q. The flexible cylinder form factor model is normalized by the particle volume accounting for an average over all possible orientations of the flexible cylinder. The model provides structural information related to the polymer's contour length, L, and the Kuhn length, b, which is the average length over which the polymer backbone is considered rigid. The scattering length density (SLD) of each component is calculated using the NIST SLD calculator[25], which gives 9.1385×10^{-7} Å^{-2} for PTMA and 4.899×10^{-6} Å^{-2} for pure d_3-MeCN, and are set parameters in the fitting of the model to the scattering of the PTMA polymer.[25] However, as the polymer became more inflexible due to increasing chain stiffness, the flexible cylinder model becomes an inadequate form factor to fit the data. For data with sharp upturns at low Q, the fractal flexible cylinder model[26] was used to characterize the structure of these polymers. The fractal model accounts for the fractal-like aggregates of the cylindrical building blocks. The fractal dimension of this model provides a statistical measurement of the cylindrical network that arises from the chain aggregation.

$$I(Q) = scale\ P(Q) + \ background \quad \text{Eq. 1}$$

The scattering curves of the small angle neutron scattering (SANS) of the neutral PTMA-X in d_3-MeCN solutions are shown in Figure 3 and the results of the fits of this data to the flexible cylinder and fractal flexible cylinder form factor are provided in Table 1. This data shows that increasing the number of TEMPO radical pendant groups on the PMMA backbone increases the coherent scattering. For samples with 20% and more TEMPO radical pendant groups the scattering curves exhibit a slight increase at low Q values ($Q < 0.007$) signifying the presence of larger

scattering objects, i.e. PTMA aggregates. However, the extent of aggregation is small and therefore the data can still be fit to the flexible cylinder form factor. The low-Q region is a representation of the overall size of the PTMA-X polymers, the mid-Q region is a representation of the stiffness of the polymer as well as the radius of the polymer chains, and the high-Q region is a direct result of the incoherent scattering.[27] ~~The fit to the flexible cylinder model provides the contour length of the PTMA chain, from which the molecular weight of the polymer can be calculated from the knowledge of the repeat units structure and the monomer molecular weight. These values are reported in Table 1 and can be compared to the molecular weight measured using GPC as a self-consistent check of the neutron scattering fitting, where good agreement is observed between these two values for all samples.~~ In the mid-Q range, the slope of the data increases slightly as the amount of TEMPO pendant radicals increases. This is a result of the increase in the local stiffness, which is quantified by the Kuhn length of the polymer, as the number of pendant radical groups increases. For PTMA-100, the sample exhibits a different shape of the scattering curve than that of the samples with lower TEMPO content. The larger upturn at low Q is a result of a larger amount of aggregation in the sample and therefore it cannot be fit to the flexible cylinder model, but must be fit to the fractal flexible cylinder model. The fractal-like aggregates can be thought of as a network produced by the assembly of the PTMA-100 flexible cylinder chains. This fractal-like aggregation is the result of intermolecular interactions between PTMA polymer chains.

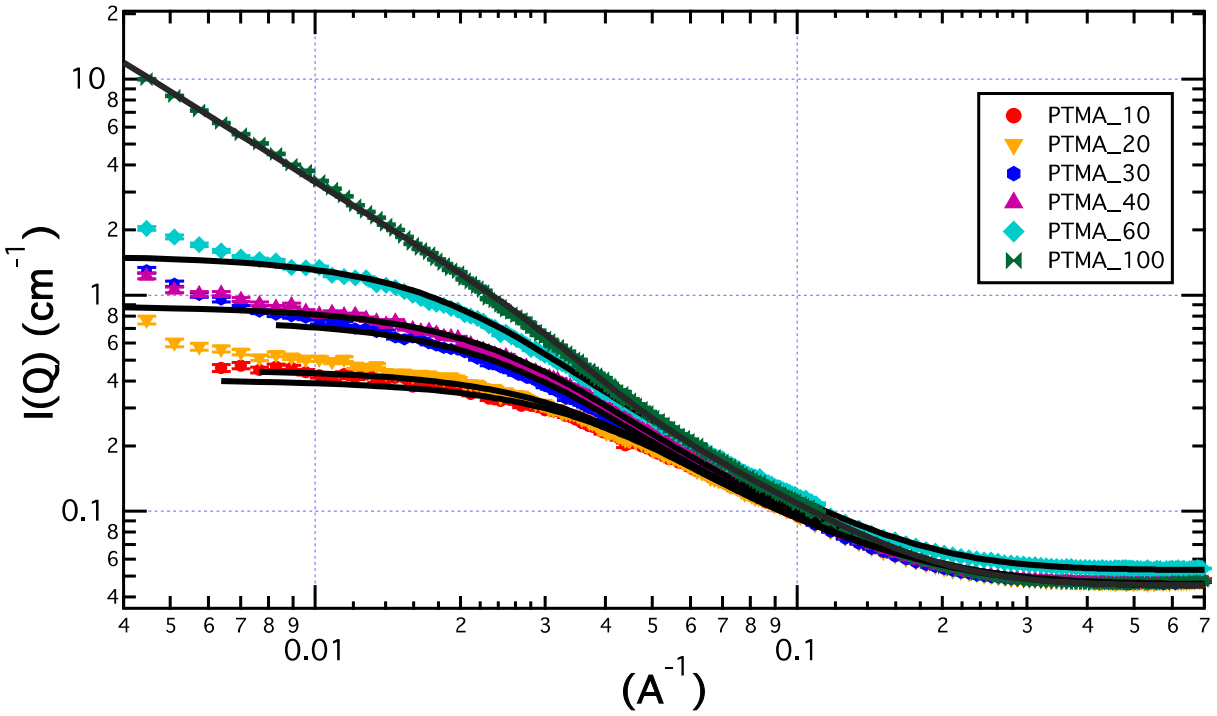

Figure 3: The SANS scattering curves of the PTMA-PMMA copolymers, with fits to the flexible cylinder model fits. PTMA-100 is fit using a fractal flexible cylinder model.

Table 1: The results of the flexible cylinder form factor fitting of the PTMA-X samples in d_3-MeCN. Molecular weights and polydispersity from GPC are reprinted from Bobela et al.[5]

Sample Name	M_n (g/mol) GPC	Polydispersity	Volume Fraction	Contour Length (Å)	Kuhn Length (Å)	Radius (Å)
PTMA-10	15,900	2.7	0.0072	261 ± 7	27.6 ± 1.3	1.8 ± 0.2
PTMA-20	24,400	2.3	0.0071	242 ± 3	38.7 ± 1.1	12.0 ± 0.1
PTMA-30	24,700	1.8	0.0071	425 ± 3	38.4 ± 0.5	2.0 ± 0.1
PTMA-40	22,000	1.8	0.0071	415 ± 4	41.7 ± 0.8	2.2 ± 0.1
PTMA-60	23,100	2.2	0.0072	556 ± 2	52.7 ± 0.6	2.5 ± 0.1
PTMA-100	17,400	1.7	0.0071	289 ± 3	92.6 ± 6.0	2.6 ± 0.4

The SANS scattering profiles of the oxidized PTMA-100 samples in d_3-MeCN, which have been dissolved and oxidized within 0.1 M $LiPF_6$ solutions (SLD of $LiPF_6$ solution is equal to $4.844x10^{-6}$ $Å^{-2}$), are shown in Figure 4. These scattering curves are also fit to the fractal flexible cylinder form factor, where the characteristic length scales from these fits are provided in Table 2. The results provided in Table 2 demonstrate that the oxidation of the chain has no overall effect on the scattering (and thus structure) of the PTMA-100. Whether PTMA-100 is dissolved in pure d_3MeCN or $LiPF_6$:d_3-MECN, the contour length, Kuhn length, and radius of the polymer is relatively unchanged. The PTMA-100 samples examined in Figure 4 vary in their extent of oxidation, which correlates structurally to the amount of oxoammonium cations per polymer chain. For example, PTMA-100 that is 18% oxidized has 82% TEMPO pendant groups that remain a radical and 18% of the TEMPO pendant groups are charged to the oxoammonium cation. The sharp slope and large low Q upturn exhibited by each PTMA-100 sample is the result of aggregation of these polymers and requires that the neutron scattering profiles be fit to the fractal flexible cylinder model. The slopes of the mid-Q region indicate that these polymers exhibit similar stiffnesses, or Kuhn lengths, regardless of the extent of oxidation of the TEMPO pendant groups. For the oxidized PTMA-100 samples, the variation of the structural characteristics of the

polymer with oxidation is minimal, indicating that the local chain structure or aggregation behavior does not change much with oxidation.

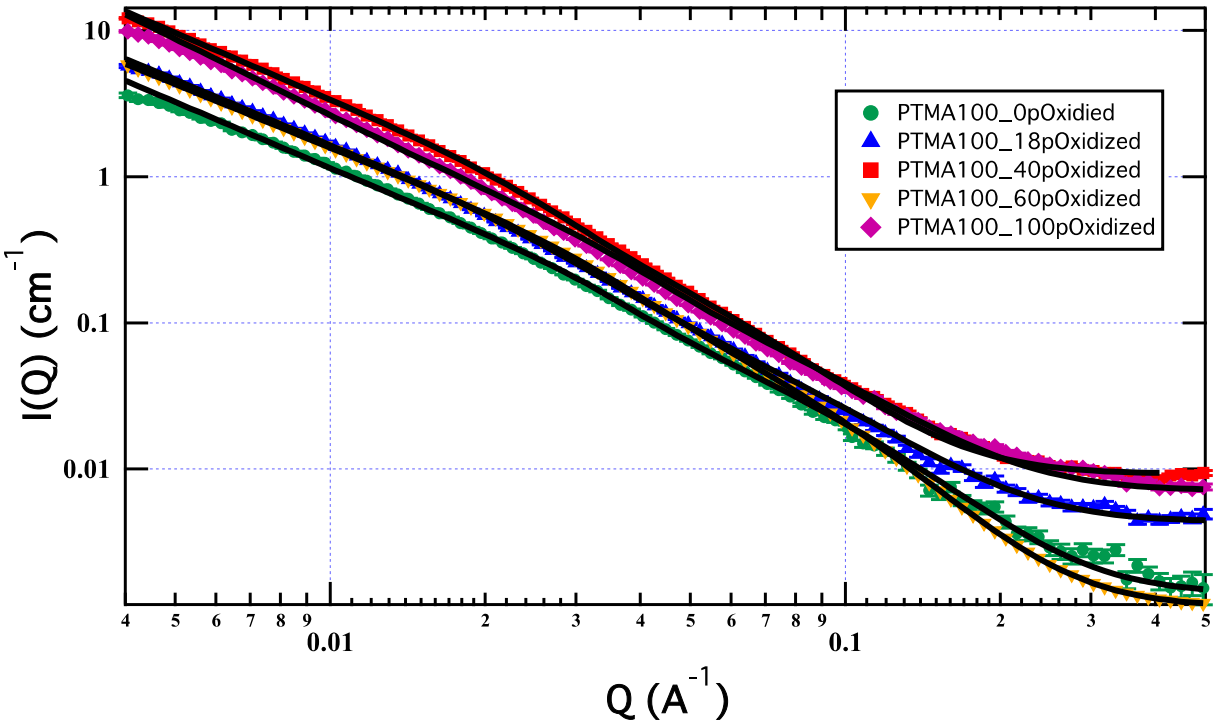

Figure 4: SANS scattering patterns for oxidized PTMA-100 in d_3-MeCN. Samples have been oxidized with $LiPF_6$ electrolyte and the data has been fitted to the fractal flexible cylinder form factor.

Table 2: The results of the fits of the PTMA-100 in d_3-MeCN oxidized samples to the fractal flexible cylinder model as a function of TEMPO oxidation.

Sample	% Oxidized	Volume Fraction	Contour Length (Å)	Kuhn Length (Å)	Radius (Å)	Fractal Dimension
PTMA-100	0	0.0071	290 ± 3	93 ± 6	2.6 ± 0.4	1.61
PTMA-100 (w/ $LiPF_6$)	0	0.0018	295 ± 3	98 ± 2	3.1 ± 0.1	1.68
	18	0.0020	381± 8	72 ± 3	3.1 ± 0.9	1.68
	40	0.0020	430 ± 4	108 ± 2	4.9 ± 0.1	1.72
	60	0.0015	299 ± 6	85 ± 4	3.7 ± 0.1	1.64
	100	0.0019	417 ± 11	86 ± 2	4.2 ± 0.1	1.76

To further examine the conformational changes of the PTMA polymers with TEMPO oxidation, the change in chain structure of PTMA-20 with oxidation is investigated. The scattering curves for PTMA-20 as a function of oxidation with the $LiPF_6$ electrolyte are provided in Figure 5, where the results of the fitting these curves to the flexible cylinder form factor are provided in Table 3. The mere presence of the $LiPF_6$ electrolyte again has no effect on the scattering curve as the contour length, Kuhn length, and radius are relatively similar for PTMA-20 with and without the $LiPF_6$ electrolyte. As the percentage of oxidized TEMPO pendant groups increases, there is a visually apparent structural change in the scattering curves which is the result of the transition of the polymer from a flexible cylinder at low oxidation to an aggregating network of flexible cylinders when the TEMPO pendant groups are entirely oxidized. The data in Table 3 shows that as the PTMA-20 becomes further oxidized from the stable radical state, the stiffness of the polymer chain increases significantly, where the Kuhn length approaches the total contour length of the polymer. It is also noted that as the oxidation of the polymer rises, the overall radius of the polymer increases from that of the polymer with neutral radicals. The scattering curve of the completely oxidized PTMA-20 in d_3-MeCN had to be fit using the fractal flexible cylinder model to account for the network of aggregates apparent in the scattering curve. Thus, the oxidation of the TEMPO

radical groups alters the structural conformation of the individually dispersed polymer chains, increasing the backbone rigidity and aggregation of the chains with an increase in oxidation.

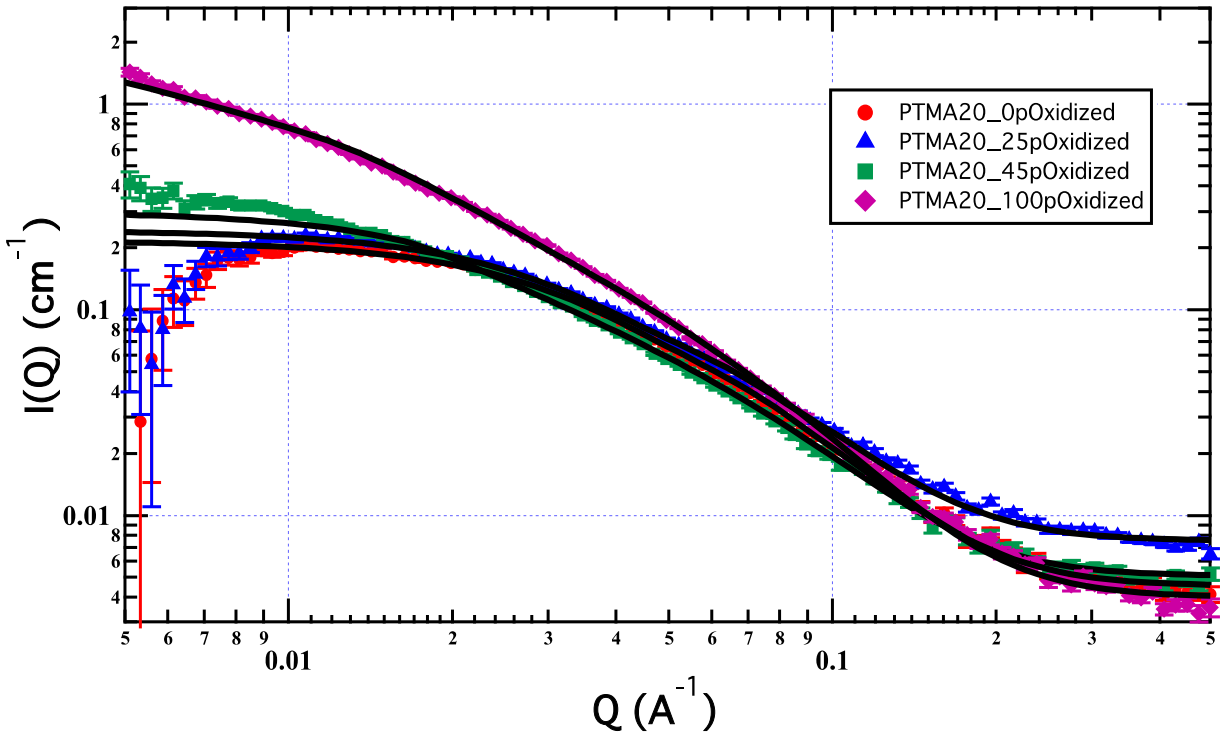

Figure 5: SANS scattering curves of oxidized PTMA-20 samples in d_3-MeCN. Samples have been oxidized with $LiPF_6$ electrolyte and fitted using either the flexible cylinder model or the fractal flexible cylinder model.

Table 3: The results of the fits of the PTMA-20 in d_3-MeCN oxidized samples to the fractal flexible cylinder model as a function of TEMPO oxidation.

Sample	% Oxidized	Scale	Contour Length (Å)	Kuhn Length (Å)	Radius (Å)	Fractal Dimension
PTMA-20	0	0.0071	242 ± 3	39 ± 1	2.0 ± 0.2	---
PTMA-20 w/ $LiPF_6$	0	0.0021	271 ± 27	48 ± 8	2.5 ± 0.2	---
	25	0.0017	241 ± 10	81 ± 6	6.7 ± 1.5	---
	45	0.0012	267 ± 5	190 ± 5	3.9 ± 0.4	---
	100	0.0015	270 ± 8	260 ± 51	4.1 ± 1.2	1

Discussion

The small angle neutron scattering experiments provide insight into the effect of increasing the pendant TEMPO radical in a PMMA polymer on the chain conformation. Organic radical batteries are often characterized by first stimulating the polymeric material, monitoring the reversibility of charging and discharging cycles, and finally determining the performance of the material by producing prototype batteries. Mostly, this research lacks knowledge on the fundamental polymeric structure and morphology of the polymer in either solution or the bulk matrix. These experiments provide an experimental test of simulation studies that indicate that the nitroxide radical concentration dictates the three-dimensional molecular packing of the polymer chain.[3,5] These molecular dynamics simulations examine the structure of radical polymers in films or solution to predict polymer aggregation and morphology and how these properties impact electron transfer distances, as well as inter- and intra- polymer chain interactions, and correlate to enhanced properties.[3–5] However, the molecular rearrangement that the amorphous polymeric materials attain during the redox process is often difficult to monitor through traditional characterization techniques. Fortunately, SANS is a suitable technique for this endeavor due to improved sample:solvent contrast through solvent deuteration. Since there is a greater need to understand the molecular rearrangements of the polymeric, radical molecule during the organic-based redox reaction, we present a comprehensive study of how the structure of the polymer is altered by the oxidation of the new organic polymeric radical materials.

Alteration of PTMA Conformation with Increasing TEMPO Radical Groups

SANS results of the neutral PTMA and PMMA copolymers clearly exhibit a structural conformation change as the density of TEMPO radicals increase on the polymer chain. The data in Figure 3 and Table 1 show that the conformation of the random copolymers of TEMPO radicals

and methyl methacrylate straighten as the TEMPO composition increases from 10% to 100%. The increase in Kuhn length of the random copolymer is a direct result of the increase in the bulky TEMPO radicals on the polymer backbone. The TEMPO units cause an increase in the steric hindrance to the rotation of the polymer chains backbone, where the interaction of the methyl groups on neighboring TEMPO radicals results in a stiffening of the polymer in solution, as shown in Figure 6 which plots the Kuhn length of the PTMA as a function of the TEMPO loading in the copolymer. The increase in radical moieties on the copolymer chain from 10% to 100% also decreases the randomness of the monomer distribution in the copolymer, forcing the backbone to stiffen to reduce the interaction between nitroxyl radical groups on the same polymer chain. Even though the PTMA backbone is relatively flexible at low loadings of TEMPO radicals as seen in Table 1, as the loading of TEMPO radicals increases, the PTMA backbone is unable to distort because the radical coupling between neighboring chains is more prevalent than the radical coupling from neighboring radicals on the same polymer chain.[3] When the PTMA polymer is completely saturated with TEMPO radicals, the polymers aggregate to form a network. These aggregates form through inter-chain interactions that evolve to optimize the distances between radicals.

These SANS studies further support the results by Bobela et al that indicate that varying the amount of TEMPO radicals in the random copolymer of PTMA will strongly influence the overall polymer conformation.[5] These molecular dynamics simulations determined that the radical-radical distances decrease from 7.5 ± 0.4Å for PTMA-20 to 5.7 ± 0.6 Å for PTMA-100. Due to the increase in Kuhn length from 27.6 Å to 92.6 Å as the TEMPO radicals loading increases from 10% to 100%, the bending of the polymer chain becomes limited, which reduces the distance between radical moieties and maximizes the number of radical interactions between neighboring

chains. Further, when the polymer chain becomes increasingly rigid, the polymer chains begin to form a network among themselves into the three primary packing motifs as suggested by Kemper et al.[3] The network formation of PTMA-100 improves the electron hoping efficiency between radical sites on neighboring polymer chains by reducing the distance between nitroxide radicals.

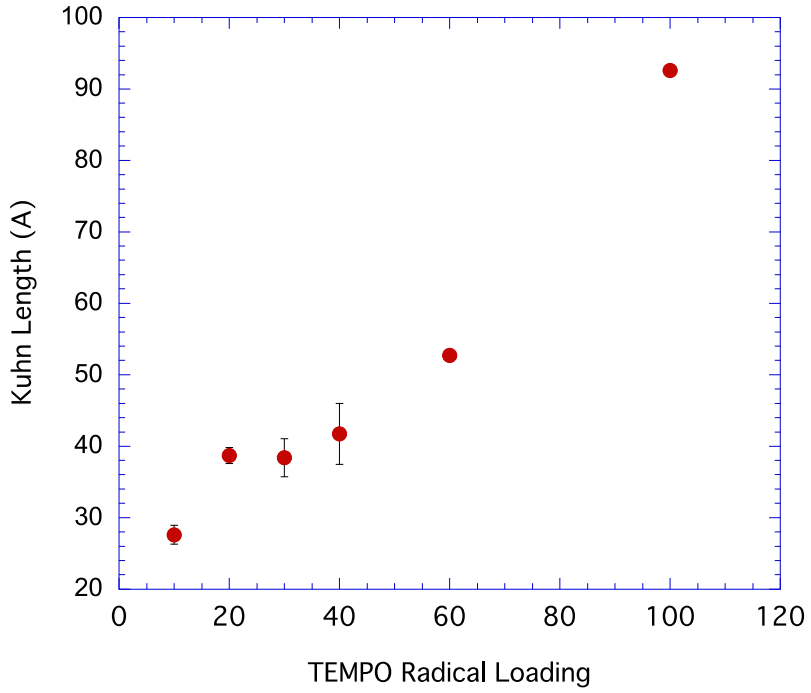

Figure 6: Change in the Kuhn Length of PTMA as a function of TEMPO radical loading on the polymer backbone.

Structural Changes of PTMA with Oxidation

The study of the structure of the oxidized copolymer reveals how the polymeric chains rearrange themselves as a result of the redox charge transfer process. Unfortunately, the reduced state of the TEMPO radical could not be studied because of sensitivity to air. This experiment mimics the reactions that the polymeric material undergoes during oxidation and monitors in situ, the changes of the polymer conformation in the redox state. As Figure 7 shows, there is little change in the rigidity of PTMA-100 as the stable TEMPO radicals are oxidized from 0% to 100%. The fact that the polymer chains aggregate at such a low volume fraction of polymer in solution

emphasizes the strong inter-polymer interactions in these samples. The increase in the number of cations on the polymer chain do not have a direct effect on the Kuhn length of the polymer or how the polymer chains organize themselves into an aggregated network, as demonstrated by the stable fractal dimension of the fractal flexible cylinder network reported in Table 2. The radius of the polymer chain also increases slightly with the oxidation of the TEMPO pendants. These results suggest that the morphology of the PTMA-100 is dominated by the steric hindrance from the bulky TEMPO pendant groups and not the oxidation of the nitroxide radicals. Kemper et al hypothesized that the strongest interactions that dominate the structure of the PTMA-100 are the interactions between the TEMPO rings that link different chains arranging themselves to reduce the distance between oxygen-nitrogen bond stacking. At this saturated TEMPO density, the impact of the oxidation of the TEMPO pendant into an oxoammonium cation is not strong enough to reassemble the aggregates of the PTMA-100 chains in a network. The aggregation of the radicals allows for almost all radicals to undergo an electron exchange interaction.[5] The high percentage of radicals decreases the susceptibility of the polymer to swelling induced reorientation.

The impact of the oxidation on the conformation of the random copolymer PTMA-20 is also analyzed to complete the overall picture of the effect of oxidation of the TEMPO radical groups on the polymer conformation. When the PTMA-20 is 100% oxidized, only 1 in every 5 repeat units of the copolymer is oxidized. This can result in a distribution of spacing between oxidized TEMPO groups. PTMA-20 in the stable radical state exhibits a flexible cylinder conformation in which the Kuhn length noticeably becomes larger as the amount of TEMPO radicals are oxidized as is documented in Figure 7. This is a result of the repulsion of the cations on the polymer chain. The scattering profiles qualitatively show that as the amount of oxidized TEMPO pendant groups increase, the PTMA chains begin to aggregate into networks as PTMA-

100 chains do, as well increasing the radius of the polymer chains. When the polymer chains are not completely saturated with bulky TEMPO pendant groups and the more flexible MMA groups are present there is a greater effect from the oxidation of the TEMPO groups on the chain conformation. In other words, the oxidization of the TEMPO pendant groups has a greater influence on the structural morphology when it is a minority component of the chain. Under these circumstances, the oxidation of distributed TEMPO groups causes the polymer chain to straighten, thus dramatically altering the chain conformation.

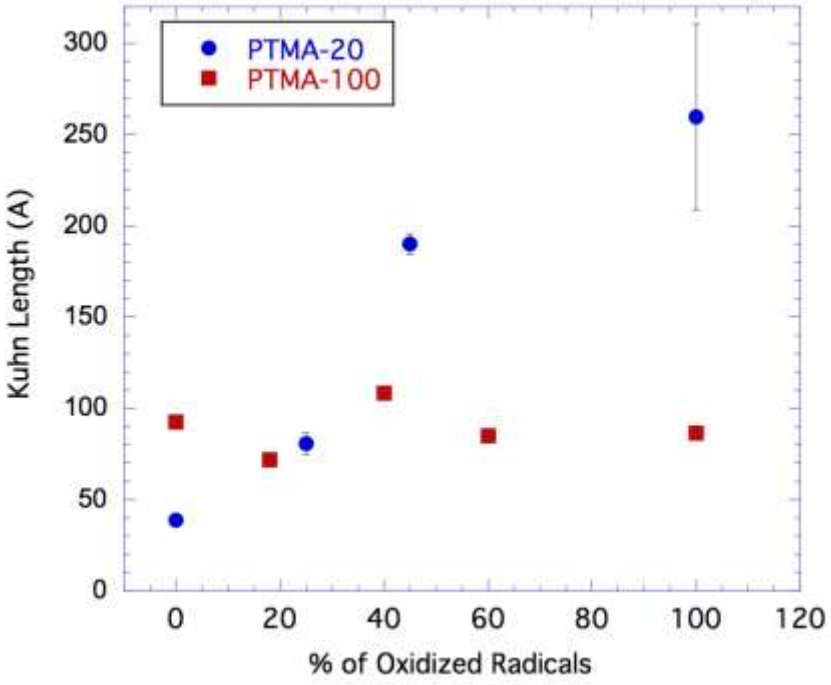

Figure 7: Change in the Kuhn length of PTMA-20 (blue circles) and PTMA-100 (red squares) as a function of radical oxidation.

Conclusion

Small angle neutron scattering offers a valuable opportunity to monitor the structural conformation changes of an organic radical polymer as a function of the density of radical pendant moieties within a polymer as well as a function of organic-based oxidation of the radical groups. Theoretical simulations predict that a random copolymers of PTMA undoubtedly undergoes a

structural change when the amount of TEMPO radicals increases on the polymer.[3,5] The SANS results agree with this interpretation, showing that the polymer becomes more rigid with an increase in the number of radical groups. This straightening is due to the increased amount of bulky pendant groups as well as increased methyl-methyl interactions between TEMPO groups. As a result of this increased polymer stiffness, the polymer chains rearrange themselves to increase the amount of radical-radical interactions between neighboring polymer chains. These inter-molecular interactions dominate because the inflexibility of the polymer chains eliminates the opportunity to form radical-radical interactions on the same chains. Thus, the larger amount of the TEMPO radicals increases the likelihood of polymer reorientation and inter-molecular interactions. The change in polymer conformation with oxidation of the TEMPO groups is also dependent on the TEMPO loading in the copolymer. When the polymer with 100% TEMPO groups, i.e. the PTMA polymer, is oxidized there is little to no change in the conformation or assembly of the polymer. However, when the polymer has a low density of TEMPO radicals, the oxidation of the radical groups into cations increases the stiffness of the polymer two-fold. Overall, these experiments further verify that the percentage of radical monomer on the polymer chain strongly influences the polymer conformation in solution. However, when the percentage of radicals is low, the polymer is more susceptible to conformational change to reduce the distance between radicals on neighboring polymer chains. This knowledge of the structural reorganization provides a foundation to optimize redox active radical polymers for device applications.

Acknowledgement

This research was supported by the Department of Energy, Basic Energy Sciences, Materials Sciences and Engineering Division. A portion of this research was also completed at ORNL's High Flux Isotope Reactor and Spallation Neutron Sources, which was sponsored by the Scientific User Facilities Division, Office of Basic Energy Sciences, US Department of Energy. This work

was authored in part by Alliance for Sustainable Energy, LLC, the manager and operator of the National Renewable Energy Laboratory for the U.S. Department of Energy (DOE) under Contract No. DE-AC36-08GO28308. The views expressed in the article do not necessarily represent the views of the DOE or the U.S. Government. The U.S. Government retains and the publisher, by accepting the article for publication, acknowledges that the U.S. Government retains a nonexclusive, paid-up, irrevocable, worldwide license to publish or reproduce the published form of this work, or allow others to do so, for U.S. Government purposes.

References

1 J.-K. Kim, G. Cheruvally, J.-W. Choi, J.-H. Ahn, S. H. Lee, D. S. Choi and C. E. Song, *Solid State Ion.*, 2007, **178**, 1546–1551.

2 Y. Liang, Z. Tao and J. Chen, *Adv. Energy Mater.*, 2012, **2**, 742–769.

3 T. W. Kemper, R. E. Larsen and T. Gennett, *J. Phys. Chem. C*, 2014, **118**, 17213–17220.

4 B. K. Hughes, W. A. Braunecker, A. J. Ferguson, T. W. Kemper, R. E. Larsen and T. Gennett, *J. Phys. Chem. B*, 2014, **118**, 12541–12548.

5 D. C. Bobela, B. K. Hughes, W. A. Braunecker, T. W. Kemper, R. E. Larsen and T. Gennett, *J. Phys. Chem. Lett.*, 2015, **6**, 1414–1419.

6 T. Janoschka, M. D. Hager and U. S. Schubert, *Adv. Mater.*, 2012, **24**, 6397–6409.

7 J. B. Goodenough and Y. Kim, *Chem. Mater.*, 2010, **22**, 587–603.

8 X. Wei, W. Xu, M. Vijayakumar, L. Cosimbescu, T. Liu, V. Sprenkle and W. Wang, *Adv. Mater.*, 2014, **26**, 7649–7653.

9 J.-K. Kim, G. Cheruvally, J.-H. Ahn, Y.-G. Seo, D. S. Choi, S.-H. Lee and C. E. Song, *J. Ind. Eng. Chem.*, 2008, **14**, 371–376.

10 W. Guo, Y.-X. Yin, S. Xin, Y.-G. Guo and L.-J. Wan, *Energy Environ. Sci.*, 2012, **5**, 5221–5225.

11 H. Chen, T. N. Cong, W. Yang, C. Tan, Y. Li and Y. Ding, *Prog. Nat. Sci.*, 2009, **19**, 291–312.

12 H. Shirakawa, E. J. Louis, A. G. MacDiarmid, C. K. Chiang and A. J. Heeger, *J. Chem. Soc. Chem. Commun.*, 1977, **0**, 578–580.

13 K. Nakahara, K. Oyaizu and H. Nishide, *Chem. Lett.*, 2011, **40**, 222–227.

14 T. Katsumata, M. Satoh, J. Wada, M. Shiotsuki, F. Sanda and T. Masuda, *Macromol. Rapid Commun.*, 2006, **27**, 1206–1211.

15 J. Qu, R. Morita, M. Satoh, J. Wada, F. Terakura, K. Mizoguchi, N. Ogata and T. Masuda, *Chem. – Eur. J.*, 2008, **14**, 3250–3259.

16 K. Oyaizu and H. Nishide, *Adv. Mater.*, 2009, **21**, 2339–2344.

17 K. Nakahara, K. Oyaizu and H. Nishide, *J. Mater. Chem.*, 2012, **22**, 13669–13673.

18 M. Kaneko, *Prog. Polym. Sci.*, 2001, **26**, 1101–1137.

19 K. Nakahara, S. Iwasa, M. Satoh, Y. Morioka, J. Iriyama, M. Suguro and E. Hasegawa, *Chem. Phys. Lett.*, 2002, **359**, 351–354.

20 L. Bugnon, C. J. H. Morton, P. Novak, J. Vetter and P. Nesvadba, *Chem. Mater.*, 2007, **19**, 2910–2914.

21 NIST - Center for Neutron Research - Small-Angle Neutron Scattering Group, https://www.ncnr.nist.gov/programs/sans/data/red_anal.html, (accessed September 5, 2017).

22 O. Arnold, J. C. Bilheux, J. M. Borreguero, A. Buts, S. I. Campbell, L. Chapon, M. Doucet, N. Draper, R. Ferraz Leal, M. A. Gigg, V. E. Lynch, A. Markvardsen, D. J. Mikkelson, R. L. Mikkelson, R. Miller, K. Palmen, P. Parker, G. Passos, T. G. Perring, P. F. Peterson, S. Ren, M. A. Reuter, A. T. Savici, J. W. Taylor, R. J. Taylor, R. Tolchenov, W. Zhou and J. Zikovsky, *Nucl. Instrum. Methods Phys. Res. Sect. Accel. Spectrometers Detect. Assoc. Equip.*, 2014, **764**, 156–166.

23 J. S. Pedersen and P. Schurtenberger, *Macromolecules*, 1996, **29**, 7602–7612.

24 W.-R. Chen, P. D. Butler and L. J. Magid, *Langmuir*, 2006, **22**, 6539–6548.

25 Neutron Activation Calculator, https://www.ncnr.nist.gov/resources/activation/, (accessed September 5, 2017).

26 R. S. Justice, D. H. Wang, L.-S. Tan and D. W. Schaefer, *J. Appl. Crystallogr.*, 2007, **40**, s88–s92.

27 S. L. Pesek, X. Li, B. Hammouda, K. Hong and R. Verduzco, *Macromolecules*, 2013, **46**, 6998–7005.

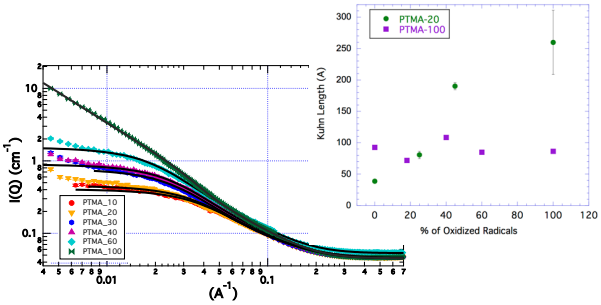

SANS provides, for the first time, unique insight into the correlation between organic radical polymer molecular structure and their assembly.